ELSEVIER

Ultrasound in Med. & Biol., Vol. 29, No. 1, pp. 65–76, 2003
Copyright © 2003 World Federation for Ultrasound in Medicine & Biology
Printed in the USA. All rights reserved
0301-5629/03/$–see front matter

PII: S0301-5629(02)00696-8

● *Original Contribution*

MP3 COMPRESSION OF DOPPLER ULTRASOUND SIGNALS

TAMIE L. POEPPING,*† JEREMY GILL,*‡ AARON FENSTER*†§ and DAVID W. HOLDSWORTH*†§

*The John P. Robarts Research Institute, London, Ontario, Canada; and †Departments of Medical Biophysics, ‡Physics and Astronomy and §Diagnostic Radiology and Nuclear Medicine, The University of Western Ontario, London, Ontario, Canada

(*Received* 6 *February* 2002; *in final form* 11 *September* 2002)

Abstract—The effect of lossy, MP3 compression on spectral parameters derived from Doppler ultrasound (US) signals was investigated. Compression was tested on signals acquired from two sources: 1. phase quadrature and 2. stereo audio directional output. A total of 11, 10-s acquisitions of Doppler US signal were collected from each source at three sites in a flow phantom. Doppler signals were digitized at 44.1 kHz and compressed using four grades of MP3 compression (in kilobits per second, kbps; compression ratios in brackets): 1400 kbps (uncompressed), 128 kbps (11:1), 64 kbps (22:1) and 32 kbps (44:1). Doppler spectra were characterized by peak velocity, mean velocity, spectral width, integrated power and ratio of spectral power between negative and positive velocities. The results suggest that MP3 compression on digital Doppler US signals is feasible at 128 kbps, with a resulting 11:1 compression ratio, without compromising clinically relevant information. Higher compression ratios led to significant differences for both signal sources when compared with the uncompressed signals. (E-mail: david.holdsworth@imaging.robarts.ca) **© 2003 World Federation for Ultrasound in Medicine & Biology.**

Key Words: **MPEG-1 Layer 3, MP3 compression, Pulsed Doppler ultrasound, Directional audio signal, Phase quadrature signal, Peak velocity, Mean velocity, Spectral width, Doppler spectral power, Carotid bifurcation, Pulsatile flow.**

INTRODUCTION

Doppler ultrasound (US) systems can provide an estimate of the instantaneous blood-flow velocity spectrum through Fourier/spectral analysis of the digitized Doppler signal. The analog Doppler signal can be easily recorded from commercial Doppler systems with the use of a conventional stereo audio digitizer. Fortunately, the Doppler US signals from most medical applications lie within the human auditory range of approximately 20 Hz to 20 kHz. This opens the door to a vast number of audio hardware and software options arising from commercial development. Some of the recording options and limitations have been discussed by Anderson (2000). One common storage method is digital audio tape (DAT), which has a capacity for up to 12 GB of uncompressed digital data, but lacks the convenience of random access media. Furthermore, Bush and Evans (1993) have shown that DAT is suitable for storing directional Doppler signals, but not for quadrature Doppler signals because a small phase shift between the two channels causes cross-talk problems, thereby requiring alternative techniques. The low cost and availability of compact disk recordable/rewritable (CD-R/RW) media and drives easily provides a robust random-access method of storing up to 650 MB of uncompressed data per disk. However, a Doppler signal digitized at 44.1 kHz and recorded with 16 bits of information per channel per datum produces over 176 kilobytes of digital stereo audio information per s; continuous acquisition of digital stereo audio data would fill nearly a single CD every hour.

Typically, in the past, it has not been standard practice to record and store Doppler signals in clinical applications. However, more recently, there is a growing need for not only recording but also transmitting Doppler data for ambulatory patient monitoring and telemedicine applications (Albright and Slater 2000; Perednia and Allen 1995; Viegas and Dunn 1998). In ambulatory patient monitoring applications, a patient may be monitored over prolonged periods of time to assess arterial blood flow

Dr. Poepping's present address is: Medical Physics, University of Edinburgh, Chancellor's Building, 49 Little France Crescent, Edinburgh, EH16 4SA, UK.

Address correspondence to D. W. Holdsworth, Imaging Research Laboratories, The John P. Robarts Research Institute, 100 Perth Drive, P.O. Box 5015, London, Ontario, N6A 5K8, Canada. E-mail: david.holdsworth@imaging.robarts.ca

following bypass grafts (Dahnoun et al. 1990), fetal heart rate and uterine contractions using wireless radiofrequency (RF) telemetry (Taylor et al. 1998) or from recordings that are later transmitted *via* telephone (Horio et al. 1998) or, potentially, for longitudinal postoperative evaluation of prosthetic heart valve function (Ramirez et al. 1988). Telemedicine applications include providing health care services or specialty consultations to remote or underserved populations (Levine and Gorman 1999; McGee and Tangalos 1994; Preston et al. 1992; Shafqat et al. 1999) and after-hours emergency echocardiography to provide quick and easy access to 24-h consultation (Trippi et al. 1996).

Research applications often require recording and storing large amounts of Doppler data for testing new algorithms or clinical applications. Examples include extended recordings of transcranial Doppler (TCD) US data for detecting emboli associated with carotid endarterectomy (Smith et al. 1995; Spencer et al. 1990), carotid stenosis (Molloy et al. 1998; Molloy and Markus 1999; Valton et al. 1995) or prosthetic heart valves (Grosset et al. 1993). Additionally, more efficient recording and storage solutions potentially may assist clinical research where Doppler data from a large number of patients must be examined, such as studies for improving Doppler US diagnostic criteria for distinguishing varying degrees of carotid stenosis (Grant et al. 1999; Huston et al. 2000; Qureshi et al. 2001). In our research applications, we routinely collect large quantities of Doppler US data while investigating the hemodynamics of the carotid bifurcation using an *in vitro* flow system, with over 5 GB of audio data collected per flow experiment (Poepping et al. 2002).

Commonly available signal compression software, such as MP3 audio compression, may offer the capability of dramatically reducing the amount of Doppler US data that must be stored and transmitted for subsequent spectral analysis in both clinical and research applications. Although typical lossless compression-decompression (codec) schemes, such as run-length encoding and the Lempel–Ziv family of algorithms, are beneficial for information storage in a wide array of applications, these codecs have a typical maximum compression ratio of about 2:1. "Lossy" codecs, such as those based on wavelet compression and algorithms designed for multimedia applications, offer higher compression ratios (10:1 and higher) at the cost of signal fidelity. These compression schemes may offer the means for reducing the handling and storage problems associated with large audio data sets, but it remains an open issue if lossy compression of Doppler US signals results in significant change to clinically relevant spectral parameters. In this study, we used an *in vitro* flow model to investigate the effect of MP3 compression on the determination of clinically significant parameters from digitized Doppler US signals. The use of a controlled *in vitro* flow model is advantageous for this type of investigation because it minimizes any confounding variability, such as physiologic variability in cardiac output, that could increase the within-group variance, potentially leading to false-negative results (*i.e.*, type II statistical errors).

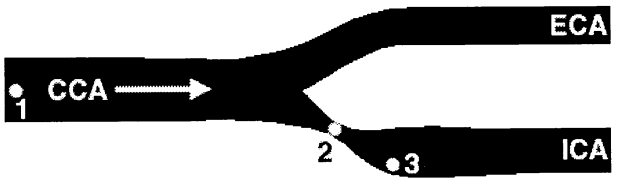

Fig. 1. Carotid bifurcation model with a 70% stenosis showing the common carotid (CCA) branching into the internal (ICA) and external (ECA) carotid arteries. The arrow indicates the direction of flow and the white dots indicate the approximate location of the three sample sites.

MATERIALS AND METHODS

Phantom

Doppler US data were recorded from the lumen of an agar-based *in vitro* flow phantom of a life-sized stenosed carotid bifurcation, which consists of the common carotid artery (CCA) branching into the internal (ICA) and external (ECA) carotid arteries. The agar phantom (Rickey et al. 1995) was fabricated using models of the carotid bifurcation, as derived by Smith et al. (1996) from x-ray arterial angiograms and a lost-material casting technique (Smith et al. 1999).

Figure 1 shows a carotid bifurcation model with a 70% stenosis (by NASCET criteria) (Fox 1993), also indicating the direction of flow and the approximate acquisition sites used here. The three acquisition sites were as follows: 1. along the center line of the 8-mm diameter CCA, 2. in the neck of the ICA stenosis, and 3. one cm downstream of the stenosis where the high-velocity jet due to the stenosis expands into the ICA. These three sites were chosen to represent varying instantaneous frequencies and frequency band widths over the cardiac cycle. Flow in the CCA is typically not turbulent, with moderate blood velocities covering a fairly small range. However, flow in the constriction or stenosis of the ICA can reach velocities in excess of 200 to 300 cm/s during peak systole, and flow downstream of the stenosis may be turbulent, with a broad spectrum of frequencies or velocities ranging from high positive velocities ($>$ 200 cm/s toward the transducer) to negative velocities (away from the transducer) due to recirculating flow.

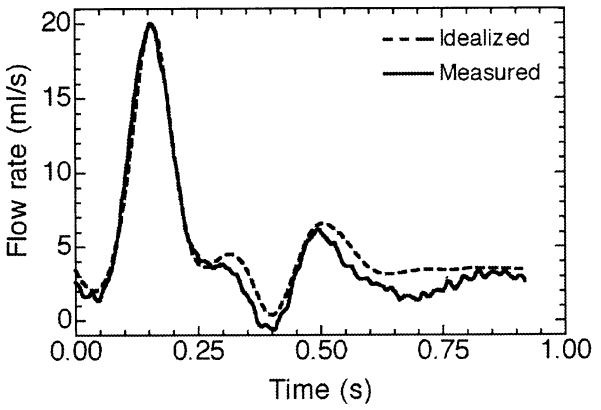

Fig. 2. Measured carotid flow waveform at the CCA inlet, along with the desired idealized waveform.

Physiologically realistic flow

A computer-controlled pump (Holdsworth et al. 1991)(UHDC Flow System, Shelley Medical Imaging Technologies, London, Canada) was used to perfuse the phantom with a pulsatile flow waveform that simulates normal common-carotid flow (Holdsworth et al. 1999). The idealized flow rate waveform was derived from *in vivo* Doppler US velocity spectra. Due to the transfer function of the flow system, the programmed waveform had to be modified to achieve the desired flow waveform at the inlet to the phantom. The resulting flow waveform was measured at the phantom inlet using an electromagnetic flowmeter (Model 322, Carolina Medical Electronics, King, NC) and is shown in comparison with the desired idealized waveform in Fig. 2. A peak flow rate of 20 mL/s (Re = 400 in CCA) was used, with a corresponding mean flow rate of 5.2 mL/s (Re = 104 in CCA).

The US blood-mimicking fluid (Ramnarine et al. 1998) was composed, by weight, of: 83.86% distilled water, 10.06% glycerol, 3.36% dextran (D4876, Sigma Chemical Co., St. Louis, MO), and 0.9% surfactant (ICI Synperonic N, EM Science, Gibbstown, NJ) with 1.82% of 5 $\pm$ 2 μm nylon particles (Orgasol 2001 UD NAT 1, Elf Atochem, Paris, France) added to provide Doppler scattering sites. The attenuation of the fluid was 0.26 dB/cm at 5 MHz, the speed of sound was 1547 m/s, and the viscosity was 4.1 $\pm$ 0.1 mPa $\cdot$ s as given by Ramnarine et al. (1998).

Ultrasound data acquisition

A clinical Doppler US system (Ultramark 8 with Access 10-PV probe, Advanced Technologies Limited, Bothell, WA) with a 5-MHz US transducer frequency was used to obtain pulsed Doppler data from within the vessel lumen at the three locations specified in Fig. 1. Doppler US signals were obtained at separate times from two sources on the US system. The phase quadrature pair can be obtained from the filtered in-phase (or direct) and quadrature signal outputs, jointly referred to as the I/Q signal pair. The separate forward and reverse, jointly referred to as F/R, flow signal components can be obtained from the left and right channels of the stereo audio headphone output. In both cases, the Doppler US signals were recorded as an audio file for off-line analysis with a stereo audio digitizer (SGI Indy, Silicon Graphics Inc., Mountainview, CA) operating at 44.1 kHz. A logic pulse provided by the computer-controlled pump allowed data acquisition to be prospectively gated. Data collected were, hence, synchronized with respect to the cardiac cycle, allowing for ensemble averaging.

A total of 10 s of cardiac-gated Doppler signal data were acquired from each of the three model sample sites. At each site, the 10-s acquisition was repeated 11 times to investigate reproducibility. A Doppler sampling volume of 10.0-mm length along the beam axis was used to incorporate a range of frequency components from across the entire velocity profile of the lumen. Doppler data were recorded with a 60° Doppler angle, 50-Hz wall filter, 100% power, 60% gain and a pulse-repetition frequency (PRF) of 22,960 Hz.

MP3 compression algorithm

The MP3 audio compression standard is a common codec, developed by the MPEG (Motion Pictures Expert Group) (Brandenburg and Stoll 1994; Hacker 2000; ISO/IEC 1993), which offers variable compression rates with good audio fidelity. An MP3 audio compression algorithm consists of three main steps: 1. breaking the original digital audio stream into fixed-length frames, 2. on a frame-by-frame basis, quantizing the spectral components and determining how to most efficiently allocate the available bits, and 3. compressing each frame using a Huffman encoding scheme. Only step 2. results in a loss of signal information. In this step, the MP3 encoder analyzes the spectral energy distribution of the audio signal by calculating a filterbank (transform) and breaking the distribution down into subbands. Mathematical models of human psychoacoustics are then applied to determine which frequencies are most significant (*i.e.*, will be most perceptible to the human ear) and which ones can be allocated fewer bits. The combined quantization and bit allocation of step 2. is the "lossy" part of the compression-decompression process.

Finally, the Huffman algorithm, used in step 3. of the MP3 encoding scheme, takes advantage of redundancies in the resulting bit stream. A set of unique codes are assigned to sequences in the audio bitstream, based on how frequently each sequence occurs. Compression of

the bitstream is accomplished by assigning shorter codes to sequences that occur frequently, and longer codes to sequences that occur less frequently.

One option that can be employed in step 2. is called joint stereo encoding, which takes advantage of similarities or correlation between the two channels for stereo audio signals to preserve bits for allocation elsewhere. The two possible modes of joint stereo encoding are mid/side stereo and intensity stereo. Mid/side mode works by encoding the mid (sum of left and right) and side (difference between left and right) channels, which may allow fewer bits to be allocated to the side band if the two channels are similar. The intensity mode works by combining the two channels into a single encoded channel for frequency subbands where the directional information is less perceptible by the human ear (and, hence, less important in audio applications). However, to ensure that directional information was not overtly compromised through joint stereo encoding, an MP3 compression algorithm that did not incorporate joint stereo encoding was chosen here.

Signal compression and postprocessing

The digitized signals were converted to MP3 format using the freely available BladeEnc software (BladeEnc, vers. 0.94.2, http://bladeenc.mp3.no/). Each of the 11 audio files was compressed at three different bit rates (128, 64 and 32 kbps), then played back (decompressed), using the freely available MPG123 software (MPG123, vers. 0.59r, http://www.mpg123.de/) into the same digital audio format. Combined with the original, uncompressed signal, a total of four signals were examined for each of the 11 audio files recorded at each of the three sites, resulting in 132 audio files for each signal source. Compression ratios of 11:1, 22:1 and 44:1 were observed for the 128, 64 and 32 kbps compression schemes, respectively. After being decompressed, each of the digital signals was then processed in an identical fashion as the original, uncompressed signal.

Postprocessing consisted of a 1024-point fast Fourier transform (FFT) with a 1024-point Hanning window and 50% overlap between consecutive 23-ms temporal windows (resulting from 1024 points with a 44.1 kHz digitization rate). Each FFT produced an estimate of the instantaneous Doppler spectrum (power vs. frequency) every 11.6 ms with a 43-Hz frequency resolution.

For the I/Q data, a single complex FFT was performed on the complex signal formed from the in-phase and quadrature signals, thereby separating the forward and reverse flow components into the positive and negative frequencies of the spectrum (Aydin and Evans 1994; Coghlan and Taylor 1976). However, with the F/R data, the forward and reverse flow components were already separated into the left and right channels. A separate FFT was performed on each of the real left and right channel signals and the positive and negative frequency components from the left and right channels, respectively, were combined to form a single frequency spectrum.

For each Doppler spectrum, an estimate of the average signal noise level was determined from the 50 frequency bins immediately below the Doppler aliasing frequency, which was determined by the PRF on the US unit (*i.e.,* for a PRF of 22,960 Hz, the 50 frequency bins cover approximately 9330 to 11,480 Hz or 287 to 350 cm/s). Subsequently, 3 times the estimated average noise level was subtracted from the entire Doppler spectrum as part of our standard noise-subtraction protocol.

The Doppler shift frequencies, f_d, were converted into blood velocities, v, using the Doppler equation:

$$v = \frac{f_d \cdot c}{2 \cdot f_t \cdot \cos\theta}, \quad (1)$$

where f_t is the transducer frequency, c is the mean speed of sound in the tissue mimic (1540 m/s), and θ is the (Doppler) angle between the transducer and the vessel. For a Doppler angle of 60°, each power vs. velocity spectrum had 1.33 cm/s velocity resolution, corresponding to the 43-Hz frequency resolution.

Each spectrum was characterized with respect to the following parameters: mean velocity (v_{mean}), peak velocity (v_{peak}), spectral width (*SW*), total integrated power and the ratio of integrated power distributed over negative vs. positive velocities (*i.e.,* reverse vs. forward flow). The positive peak velocity was defined in this study as the velocity corresponding to 90% of the power integrated over positive velocities after noise subtraction. The spectral width was defined as the full width at half of the maximum power. The spectral width is typically used in flow measurements as an indicator of disturbed flow, which is often associated with stenosed arteries, and may vary slightly with different spectral analysis techniques (Keeton et al. 1997).

This spectral characterization was repeated for each spectrum (*i.e.,* every 11.6 ms) so that each of the above parameters was traced out as a function of time for 10 full cardiac cycles, where each cardiac cycle (0.92 s) consisted of 79 spectra. The ensemble average (one average cardiac cycle) was then determined for both v_{peak} and v_{mean} by averaging 10 successive cardiac-gated cycles. Also, the time-averaged value (averaged over the full 9.2 s) was determined for each derived spectral parameter.

Repeated-measurements, one-way analysis of variance (ANOVA) with a Tukey *post hoc* analysis (Zar 1984) was performed on the four sets (uncompressed

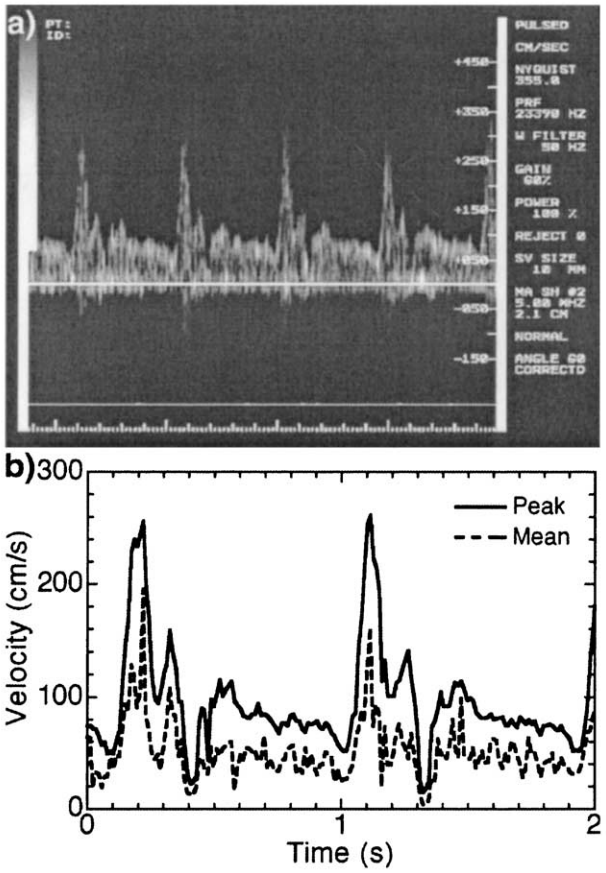

Fig. 3. Doppler data from a site within the ICA: (a) a typical Doppler spectral display from the Ultramark 8, (b) peak (—) and mean (– – –) velocity traced over three cardiac cycles derived from uncompressed Doppler US I/Q data.

plus 3 compression rates) of 11 time-averaged values (from 11 acquisitions) for each of the five spectral parameters, to determine any significant differences ($p < 0.05$) between the spectra derived from the uncompressed and decompressed signals. The use of a repeated-measurements technique increased the statistical power of the analysis by recognizing the correlation between values derived from corresponding uncompressed and decompressed data files.

RESULTS AND DISCUSSION

Example data shown in Figs. 3 to 7 were selected from site 3 (as marked in Fig. 1) downstream of the stenosis in the ICA, because this was expected to be the most difficult and, hence, limiting, case due to the large inherent dynamic range of the velocities at this site.

Peak and mean velocity waveforms

Figure 3 shows Doppler spectral data obtained from the acquisition site within the ICA (site 3 in Fig. 1). A typical Doppler screen display from the clinical US unit is shown in Fig. 3a. Figure 3b shows v_{peak} and v_{mean} traced out over several cardiac cycles derived from off-line spectral analysis of a typical uncompressed I/Q signal pair.

Similarly, v_{peak} and v_{mean} waveforms were derived from the decompressed data files. However, all the velocity waveforms derived from decompressed Doppler

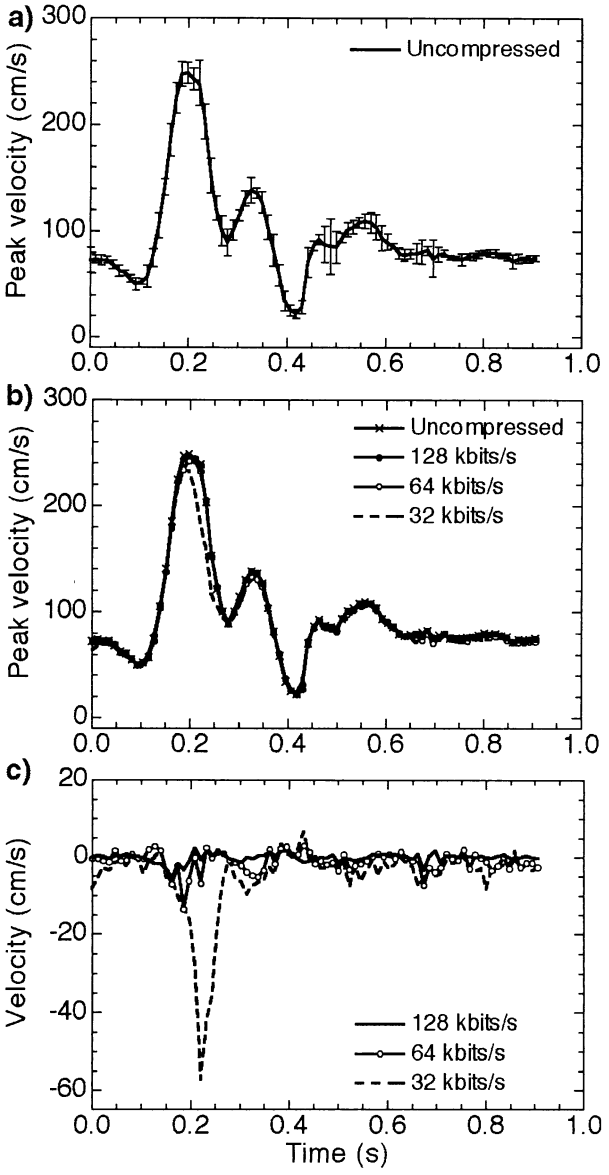

Fig. 4. (a) Ensemble-averaged v_{peak} waveform for an uncompressed data file of in-phase and quadrature (I/Q) signals with SD shown at each point derived from the 10 cardiac cycles. (b) Ensemble-averaged v_{peak} waveforms corresponding to the four compression schemes, and (c) the residuals for each of the decompressed-data waveforms after subtracting the uncompressed-data waveform.

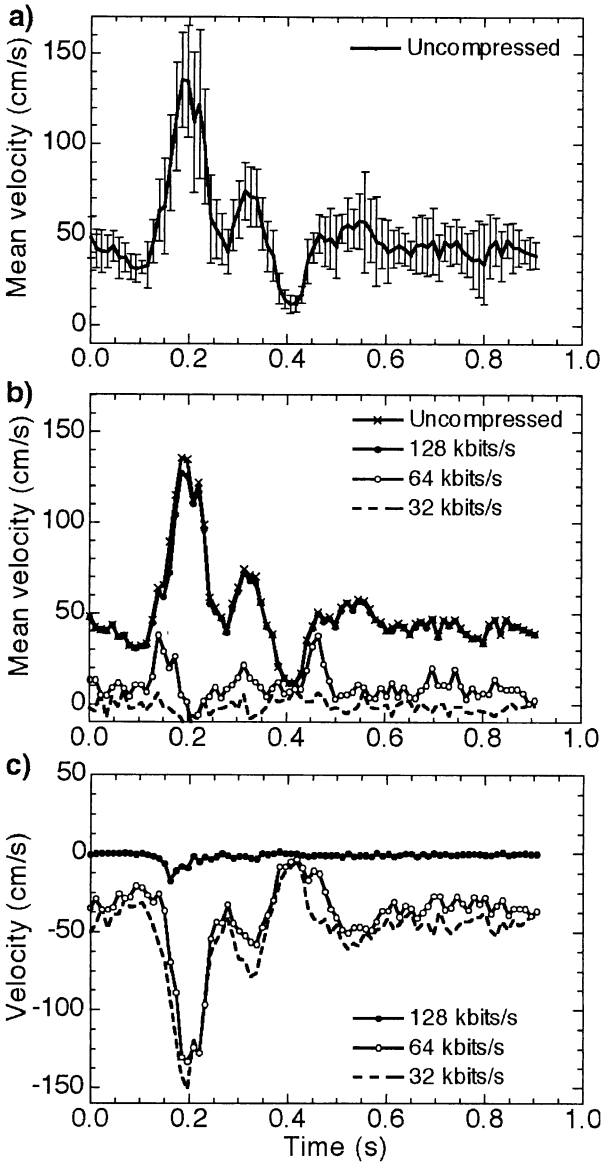

Fig. 5. (a) Ensemble-averaged v_{mean} waveform for an uncompressed I/Q data file with SD shown at each point derived from the 10 cardiac cycles. (b) Ensemble-averaged v_{mean} waveforms corresponding to the four compression schemes, and (c) the residuals for each of the decompressed-data waveforms after subtracting the uncompressed-data waveform.

data exhibited erroneous results at the beginning of the waveform and a consistent temporal lag of approximately 23 ms with respect to the uncompressed data. This delay was an artefact introduced during the conversion to MP3 format when the signal data were broken into individual frames. The temporal lag was eliminated by discarding the first 1024 points of the decompressed digital signal before analysis.

The average v_{peak} waveform from an ensemble of

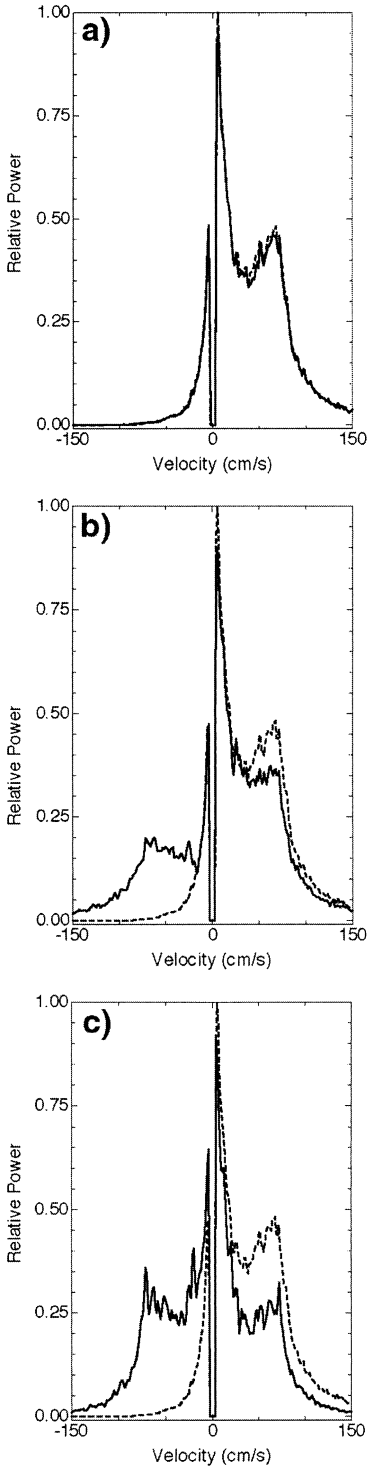

Fig. 6. Comparison of power spectra, averaged over 10 cardiac cycles, corresponding to the four compression schemes applied to a representative pair of Doppler US I/Q signals acquired within the ICA (site 3 in Fig. 1). The power spectrum for the uncompressed data are shown (· · · ·) for comparison with the spectra derived from the corresponding signal compressed at (a) 128 kbps, (b) 64 kbps and (c) 32 kbps. The power spectra have been normalized relative to maximum power within the set.

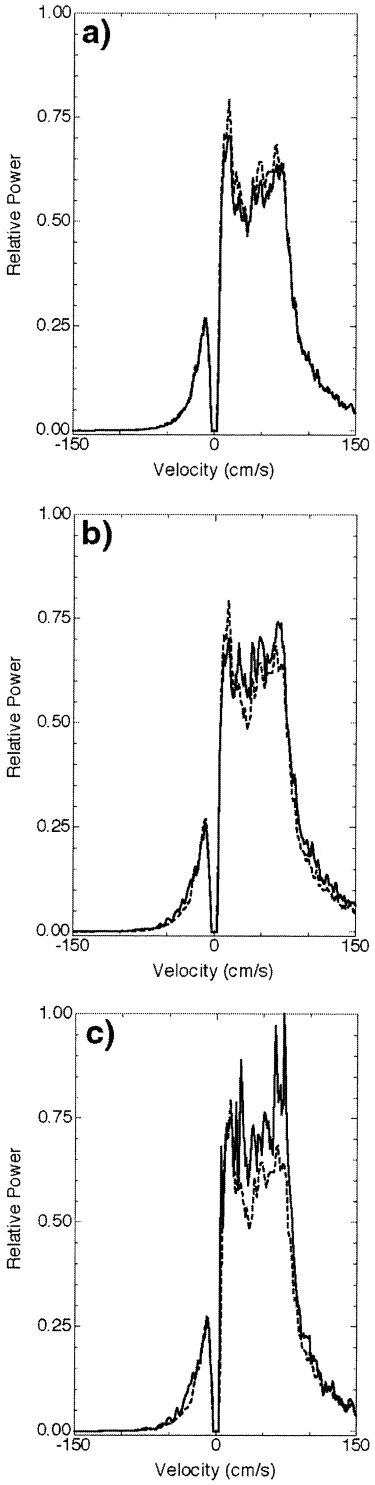

Fig. 7. Comparison of power spectra, averaged over 10 cardiac cycles, corresponding to the four compression schemes applied to a representative pair of Doppler US F/R signals acquired within the ICA (site 3 in Fig. 1). The power spectrum for the uncompressed data are shown (· · · ·) for comparison with the spectra derived from the corresponding signal compressed at (a) 128 kbps, (b) 64 kbps and (c) 32 kbps. The power spectra have been normalized relative to maximum power within the set.

10 successive cardiac cycles of uncompressed quadrature data are shown in Fig. 4 along with the SD in the 10 contributing values at each time-point shown as error bars. The SDs, which correspond to the typical fluctuation from cycle to cycle at each time-point in the cardiac cycle, ranged from 2 to 26 cm/s. Figure 4b shows the ensemble-averaged v_{peak} waveform derived from the uncompressed I/Q signal pair compared to the v_{peak} waveform derived from the three corresponding decompressed I/Q signals. The point-by-point residual errors, or differences between each decompressed v_{peak} waveform and the uncompressed waveform, are shown in Fig. 4c. Compressed spectra primarily resulted in underestimation of v_{peak}, with maximum residual velocity errors of 5, 14 and 57 cm/s for 128, 64 and 32 kbps compression, respectively. For 128 and 64 kbps, these residual errors are well within the range of the cycle-to-cycle fluctuations in the uncompressed I/Q data, as indicated by the error bars in Fig. 4a.

Similarly, Fig. 5 shows the corresponding ensemble-averaged v_{mean} waveforms and residual plot, demonstrating much larger SDs in the v_{mean} from uncompressed I/Q data (Fig. 5a) and greater velocity underestimation in the decompressed data (Fig. 5c). For $v_{mean,}$ the SDs in the uncompressed I/Q data ranged from 4 to 41 cm/s, and the maximum residual velocity errors were 17, 133 and 151 cm/s for 128, 64 and 32 kbps compression, respectively. The larger variance in v_{mean} relative to v_{peak} suggests that the v_{peak} is less sensitive to noise than the v_{mean}, as has been shown previously by Evans et al. (1989). The residual errors for v_{mean} were also larger than for v_{peak}, especially for the lower bit rate compression. However, for 128 kbps compression, the residual errors were still within the cycle-to-cycle SDs of the uncompressed data.

Similar results were obtained for the F/R data, where the SDs in the uncompressed F/R data ranged from 3 to 28 cm/s for v_{peak} and 4 to 39 cm/s for v_{mean}. The maximum residual velocity errors for 128, 64 and 32 kbps compression, respectively, were 7, 10 and 42 cm/s in v_{peak} and 5, 10 and 40 cm/s in v_{mean}, which are considerably lower than the corresponding values from the I/Q data for the lower bit rate compression.

ANOVA and post hoc analysis on time-averaged parameters

The time-averaged spectral parameters for the four compression schemes and the results of the Tukey *post hoc* analysis comparing the decompressed-data and uncompressed data parameters are summarized in Table 1 for both the I/Q and F/R signals. The *post hoc* analysis was performed on spectral parameters derived from the decompressed data after eliminating the initial 1024 sig-

Table 1. Results averaged over 11 acquisitions of 10 cardiac cycles of Doppler data corresponding to three acquisition sites, two source types (I/Q and F/R) and four compression schemes. The SD in the 11 time-averaged values is given in parentheses. I/Q = data from the in-phase and quadrature signal pair, F/R = data from forward and reverse flow signal pair. Significant differences (p values) are noted.

Signal type	Site	Uncompressed	128 kbps	64 kbps	32 kbps
Backward/forward power ($\times 10^{-2}$)					
	CCA	0.18 (0.10)	0.20 (0.12)	1.15 (0.15)*	2.76 (0.25)*
I/Q	STENOSIS	1.76 (0.17)	2.37 (0.16)	44.44 (1.99)*	91.52 (3.89)*
	ICA	12.04 (1.71)	12.80 (0.76)	49.43 (37.39)*	94.43 (82.39)*
	CCA	0.16 (0.02)	0.17 (0.02)	0.33 (0.03)*	0.39 (0.04)*
F/R	STENOSIS	1.46 (0.10)	1.54 (0.10)	2.36 (0.11)*	1.89 (0.11)*
	ICA	9.09 (1.21)	9.17 (1.94)	9.22 (3.25)	9.26 (2.88)
Integrated power ($\times 10^{5}$)					
	CCA	2.04 (0.11)	2.02 (0.10)	1.93 (0.09)	1.91 (0.09)
I/Q	STENOSIS	0.45 (0.22)	0.43 (0.17)	0.49 (0.19)	0.54 (0.26)*
	ICA	1.25 (0.05)	1.21 (0.05)	1.41 (0.06)*	1.38 (0.06)
	CCA	10.00 (0.48)	9.92 (0.48)	9.54 (0.49)	9.44 (0.46)
F/R	STENOSIS	2.98 (0.12)	2.84 (0.13)	3.12 (0.14)	3.72 (0.18)*
	ICA	7.13 (0.28)	6.78 (0.28)	7.88 (0.32)*	8.39 (0.33)*
Spectral width (cm/s)					
	CCA	4.84 (0.10)	4.85 (0.08)	4.83 (0.09)	5.69 (0.25)*
I/Q	STENOSIS	17.58 (0.56)	17.69 (0.62)	95.27 (3.75)*	133.17 (2.77)*
	ICA	56.83 (1.94)	57.83 (1.73)	82.61 (3.12)*	92.28 (2.31)*
	CCA	4.72 (0.05)	4.73 (0.07)	4.75 (0.07)	4.80 (0.07)
F/R	STENOSIS	16.32 (0.41)	16.06 (0.51)	19.54 (0.85)*	18.91 (0.46)*
	ICA	54.88 (1.86)	54.24 (2.06)	53.93 (1.80)	47.43 (1.94)*
Mean velocity (cm/s)					
	CCA	13.41 (0.06)	13.39 (0.07)	12.87 (0.08)*	11.94 (0.17)*
I/Q	STENOSIS	81.09 (0.82)	79.75 (0.83)*	26.28 (0.81)*	1.18 (0.75)*
	ICA	47.12 (0.84)	45.83 (0.88)†	13.03 (0.80)*	−1.73 (0.34)*
	CCA	13.60 (0.09)	13.59 (0.09)	13.59 (0.09)	15.51 (0.09)
F/R	STENOSIS	82.56 (0.62)	82.18 (0.58)	80.30 (0.65)*	82.50 (0.71)
	ICA	52.22 (1.20)	52.02 (1.15)	52.63 (1.11)	50.90 (1.46)
Peak velocity (cm/s)					
	CCA	15.82 (0.10)	15.86 (0.10)	15.88 (0.11)	15.93 (0.10)
I/Q	STENOSIS	100.56 (1.04)	100.50 (0.99)	100.68 (0.98)	99.74 (0.92)
	ICA	93.63 (0.94)	93.29 (1.01)	91.53 (0.88)*	85.73 (1.10)*
	CCA	15.95 (0.09)	15.96 (0.10)	16.11 (0.10)	16.19 (0.10)
F/R	STENOSIS	101.14 (0.84)	101.29 (0.83)	102.95 (0.95)*	101.24 (0.87)
	ICA	95.26 (1.13)	95.18 (1.22)	97.04 (1.36)*	91.91 (1.32)*

Note that recorded signal levels were different for I/Q and F/R acquisitions, so it is not pertinent to compare arbitrary power levels between the two source types. *$p < 0.01$; †$p < 0.05$.

nal points to avoid the erroneous data from the MP3 codec delay mentioned earlier. Table 1 shows mean values of the time-averaged power ratio, integrated power, spectral width, v_{mean}, and v_{peak}, where each value is the overall average from 11 time-averaged values, derived from 11 audio files of 10 cardiac cycles each. The SD in the 11 time-averaged values is given in brackets. Cases where the 11 time-averaged values from the decompressed data were determined to be significantly different ($p < 0.05$) from the corresponding values for the uncompressed data are noted in the table.

Power ratio Note that, for the uncompressed files, generally a small fraction (*i.e.*, $\leq 1\%$) of the power arose from negative velocities (reverse flow) except in the ICA, which included some recirculating or reverse flow (up to 12% of the power relative to forward flow) as seen in Table 1. For both signal sources, this power ratio was preserved at 128 kbps compression with no significant differences from the uncompressed data. However, significant differences were seen with the 64 and 32 kbps compression.

For the I/Q data, this appears to be due to a loss of the precise phase relationship between frequency components in the two channels. This loss of phase information results in ambiguity regarding direction of flow relative to the transducer. Figure 6 shows the power spectra for an I/Q data file acquired from site 3 within the ICA. Fig. 6a, b and c correspond to the 128, 64 and 32 kbps decompressed data (—), respectively, compared in each case to the uncompressed data (– – –). The power drop observed around the origin is due to the 50-Hz wall filter of the Ultramark 8, which filtered out the high power signal at low frequencies (−50 to 50 Hz) arising from the tissue mimic and vessel wall.

Notice that, when directional information was compromised with 64 kbps compression, power arising from positive velocities was incorrectly assigned to negative velocities, which increased the power ratio. At 32 kbps, there appears to be a nearly complete loss of directional information that resulted in a power distribution evenly split between positive and negative velocities, as indicated in Table 1 by a power ratio near unity.

Similarly, Fig. 7a, b and c shows the power spectra for an F/R data file acquired at the same site. However, in contrast to Fig. 6, there appears to be very little increase in the power ratio for the F/R data, although the differences were still statistically significant at lower bit rates.

For the F/R data, essentially very little bandwidth is required for the reverse flow component (right audio channel or negative velocities) because most of the signal power is from forward flow (left audio channel or positive velocities). However, for the I/Q data, each channel is comprised of both forward and reverse flow components with the phase between channels providing the directional information. Thus, the two channels have equal amounts of related, but different, signal information and, therefore, require twice the band width. Hence, compression of the I/Q data not only presents a greater challenge with respect to band width than does the F/R data, but any compromise of frequency data in one channel also comes at a greater cost if it means a loss of directional information too.

Integrated power Despite the differences in the power ratio, the integrated power, which corresponds to the area under the power spectrum, appeared to be fairly well preserved as shown in Table 1. For normal audio applications of MP3 compression, this would be highly desirable to maintain the relative volume. Differences in integrated power were insignificant in most cases, except with low bit rates (high compression ratios) and broad band width signals, when the effect of large degrees of signal quantization, due to allocation of fewer bits to frequency subbands, led to significant differences.

Spectral width No significant differences were observed in the spectral width at 128 kbps, as shown in Table 1. With 64 and 32 kbps compression of the I/Q data, the spectral width increased drastically in several cases due to the loss of directional information and, hence, increased power from the negative velocities. Much smaller differences were observed for the F/R data.

Mean velocity With the 128 kbps compression of F/R data, no significant differences were observed in v_{mean} in the CCA, as shown in Table 1. However, small, but statistically significant, differences were observed for the I/Q data from the ICA and stenosis, with a mean difference of 1.3 cm/s, which is less than a 3% difference relative to the uncompressed data. Recall that the frequency resolution of 43 Hz led to a 1.33 cm/s velocity resolution; thus, the observed difference corresponds approximately to a single discrete step in velocity.

The compromise of directional information with 64 and 32 kbps led to very significant differences in the power distribution, as shown by the power ratio, thus also affecting v_{mean}. The even split in power distribution over positive and negative velocities for 32 kbps compression, as indicated by a power ratio near one, was also reflected with a v_{mean} near zero. For the F/R data, no significant differences were observed in v_{mean} with one exception (*i.e.*, 64 kbps, stenosis).

Peak velocity Finally, as shown in Table 1, no significant differences were observed in the time-averaged peak velocity values derived from the 128 kbps decompressed data compared to the uncompressed data. Despite showing statistically significant differences with 64 kbps compression, the peak velocity values were still remarkably similar to the uncompressed data, as shown in Fig. 5 and Table 1, due to the good preservation of the integrated power from which the peak velocity was determined.

DISCUSSION AND SUMMARY

128 kbps compression

For the I/Q data, no significant differences were observed in the time-averaged values of v_{peak}, spectral width, integrated power or power ratio with 128 kbps compression. Although no significant differences were observed in the time-averaged value of v_{mean} in the CCA, relatively small, yet statistically significant, differences resulted in the data from the two high-velocity locations (sites 2 and 3 in the stenosis and ICA). However, these differences were equal to approximately a single discrete increment in velocity and were well within the point-by-point SDs (shown as error bars in Fig. 4) due to the cycle-to-cycle fluctuations in the v_{mean} waveforms. The v_{peak} and v_{mean} waveforms also agreed well qualitatively with those from the uncompressed I/Q data.

For the F/R data, no significant differences were observed in any of the time-averaged values for the 128 kbps decompressed data relative to uncompressed.

These results suggest that MP3 compression on digital Doppler US signals is feasible at 128 kbps, with a resulting 11:1 compression ratio, without compromising clinically relevant information.

64 kbps compression

The compromise of Doppler directional information led to significant differences in the time-averaged values from the decompressed I/Q data compared to the uncompressed data in 10 of the 15 cases tested, with only v_{peak} and the integrated power being well preserved in most cases. Although the v_{peak} waveform appeared to agree well with the uncompressed data, the v_{mean} waveform did not. Given the highly significant errors arising in most cases, MP3 compression of Doppler I/Q signals at 64 kbps cannot be recommended.

Although the differences between the uncompressed and decompressed F/R data were generally small with 64 kbps compression, they were still significantly different in 6 of the 15 cases tested. The relatively small, yet significant, differences suggest that perhaps 64 kbps compression of F/R data are feasible for certain applications but should be used with caution.

32 kbps compression

With 32 kbps compression, the extreme demands for reduced band width led to significant differences from the uncompressed data in nearly all (11 of 15) of the considered spectral parameters for the I/Q data and in 7 of 15 cases for the F/R data. Again, the large differences in the spectral parameters in most cases indicate that MP3 compression of Doppler signals at 32 kbps should not be used.

Limitations

The peak velocities were derived from the spectra using one particular technique of peak velocity estimation that is based on the integrated power. Given the overall preservation of the power spectrum with 128 kbps compression, other peak velocity estimators based on the integrated power (Mo et al. 1988; Steinman et al. 2001) should also continue to work at 128 kbps. Problems may arise at lower bit rates (higher compression ratios) due to the redistribution of the power spectrum, or with other peak velocity estimation techniques that do not use the integrated power. However, with MP3 compression, low-power spectral components are often rounded down to zero during the quantization step. Thus, MP3 compression acts like a filter to reduce low-power signals, such as noise, especially in the upper frequency bins. This may actually improve performance of some peak velocity followers. Future work, however, could include testing of other peak velocity followers and spectral analysis techniques.

It should also be noted that although Doppler US signals are coincidentally, and conveniently, within the human auditory range, MP3 compression was not specifically designed and, hence, not optimized for US data. The application of human psychoacoustic models may pose a potential disadvantage. For example, because the human ear is logarithmically sensitive to frequencies, some MP3 compression algorithms impose band limitations where frequencies are decimated above some cutoff, typically 16 kHz. Additionally, MP3 algorithms take advantage of the masking effect, where one sound is masked by a much louder sound, by decimating the less audible sound. Hence, MP3 compression may not be the ideal compression scheme for Doppler signals. However, MP3 compression is highly suitable in that it is adaptive to the instantaneous spectrum, which is important for pulsatile flow data, and it gives the advantage of a huge resource of accessible software and off-the-shelf hardware.

Optimization of a compression algorithm specifically for US data would ensure that channel separation is never intentionally compromised (*i.e.*, features like joint-stereo encoding are not implemented) and no band limitations are imposed below the Nyquist frequency limit inherent to the PRF.

SUMMARY

Commonly available signal compression software, such as MP3 audio compression, offer the capability to dramatically reduce the amount of Doppler US data that must be stored and transmitted for subsequent spectral analysis. We have described a quantitative analysis of the effects of MP3 compression on clinically important Doppler velocity parameters. The investigation was carried out in a controlled *in vitro* model, thereby removing the confounding physiologic variability (in cardiac output, for example) inherent to *in vivo* data. This variability would otherwise lead to type II (or false-negative) statistical errors due to an increased within-group variance. However, we expect the results to be transferable to *in vivo* data, as well. Our results indicate that an order-of-magnitude reduction in file size could be achieved with MP3 audio compression at 128 kbps without suffering any critical loss of information.

These results have implications for research protocols that acquire Doppler US data over multiple cardiac cycles. In our own research program, we routinely collect 10 s of quadrature data at each of 3000 sample points within a model, resulting in over 5 Gbytes of uncompressed data for each experiment (Poepping et al. 2002). With MP3 compression, the results of such an investigation could be reduced to less than 500 Mbytes for easy storage on a single compact disk (CD-R). Additionally, the recent availability of real-time MP3 hardware encoders may make routine clinical implementation of MP3 compression feasible during clinical investigations.

Future work

One of the obvious applications for Doppler signal compression would be for transcranial Doppler (TCD) US used for monitoring patients over an extended period of time for high-intensity transient signals (HITS) corresponding to emboli. However, because this analysis did not include TCD data, future work would be needed to ensure that the HITS of various durations and intensities are preserved with MP3 compression.

Our goal was to demonstrate the feasibility of using lossy MP3 compression on digital Doppler US data. To achieve this, we have chosen one particular MP3 encoder, the freely available BladeEnc, because it does not incorporate stereo redundancy encoding (such as joint-stereo encoding where the left and right channels are stored together for some frequencies) to conserve band width, which would inherently lead to a loss of Doppler directional information for either I/Q or F/R signals. Although not all MP3-compression algorithms are identical, they all should comply with the MPEG-I-layer 3 specification (ISO/IEC 1993) laid out by the International Standards Organization (ISO). However, future work could include the testing of other MP3 encoders or other types of compression schemes.

Acknowledgments—The authors acknowledge Dr. Richard Rankin for his helpful discussions and thank ATL for providing the Ultramark 8 US unit. Financial support is acknowledged from the Heart and Stroke Foundation of Ontario (Grant #T-4383), the Heart & Stroke Foundation of Canada (Career Investigator funding of D. W. Holdsworth) in conjunction with Canadian Institutes of Health Research (CIHR/HSFC Partnership Graduate Scholarship of T. L. Poepping), and the John P. Robarts Research Institute (Graduate Student Award of T. L. Poepping).

REFERENCES

Albright K, Slater SG. Medical devices in the home: Present and future applications. Caring 2000;19:36–38.

Anderson T. Recording and reproduction of Doppler signals and colour Doppler images. In: Evans DH, McDicken WN, eds. Doppler US: Physics, instrumentation, and clinical applications. Chichester, UK: John Wiley & Sons, Ltd., 2000:405–414.

Aydin N, Evans DH. Implementation of directional Doppler techniques using a digital signal processor. Med Biol Eng Comput 1994;32: S157–S164.

Brandenburg K, Stoll G. ISO-MPEG-1 audio—A generic standard for coding of high-quality digital audio. J Audio Eng Soc 1994;42: 780–792.

Bush G, Evans DH. Digital audio tape as a method of storing Doppler ultrasound signals. Physiol Meas 1993;14:381–386.

Coghlan BA, Taylor MG. Directional Doppler techniques for detection of blood velocities. Ultrasound Med Biol 1976;2:181–188.

Dahnoun N, Thrush AJ, Fothergill JC, Evans DH. Portable directional ultrasonic Doppler blood velocimeter for ambulatory use. Med Biol Eng Comput 1990;28:474–482.

Evans DH, Schlindwein FS, Levene MI. The relationship between time averaged intensity weighted mean velocity, and time averaged maximum velocity in neonatal cerebral arteries. Ultrasound Med Biol 1989;15:429–435.

Fox AJ. How to measure carotid stenosis. Radiology 1993;186:316–318.

Grant EG, Duerinckx AJ, El Saden S, et al.. Doppler sonographic parameters for detection of carotid stenosis: Is there an optimum method for their selection? Am J Roentgenol 1999;172:1123–1129.

Grosset DG, Georgiadis D, Kelman AW, Lees KR. Quantification of ultrasound emboli signals in patients with cardiac and carotid disease. Stroke 1993;24:1922–1924.

Hacker S. MP3: The definitive guide. Cambridge, MA: O'Reilly, 2000.

Holdsworth DW, Norley CJ, Frayne R, Steinman DA, Rutt BK. Characterization of common carotid artery blood-flow waveforms in normal human subjects. Physiol Meas 1999;20:219–240.

Holdsworth DW, Rickey DW, Drangova M, Miller DJ, Fenster A. Computer-controlled positive displacement pump for physiological flow simulation. Med Biol Eng Comput 1991;29:565–570.

Horio H, Murakami M, Chiba Y, Inada H. Fetal monitor for non-stress-test screening at home. Biomed Instrum Technol 1998;32:39–47.

Huston J III, James EM, Brown RD Jr, et al.. Redefined duplex ultrasonographic criteria for diagnosis of carotid artery stenosis. Mayo Clin Proc 2000;75:1133–1140.

ISO/IEC International standard ISO 11172–3. Information technology–Coding of moving pictures, and associated audio for digital storage media at up to about 1.5 Mbits/s-Part 3: Audio. Geneva, Switzerland: ISO/IEC 1993.

Keeton PI, Schlindwein FS, Evans DH. A study of the spectral broadening of simulated Doppler signals using FFT and AR modelling. Ultrasound Med Biol 1997;23:1033–1045.

Levine SR, Gorman M. "Telestroke: " The application of telemedicine for stroke. Stroke 1999;30:464–469.

McGee R, Tangalos EG. Delivery of health care to the underserved: Potential contributions of telecommunications technology. Mayo Clin Proc 1994;69:1131–1136.

Mo LY, Yun LC, Cobbold RS. Comparison of four digital maximum frequency estimators for Doppler ultrasound. Ultrasound Med Biol 1988;14:355–363.

Molloy J, Markus HS. Asymptomatic embolization predicts stroke and TIA risk in patients with carotid artery stenosis. Stroke 1999;30: 1440–1443.

Molloy J, Khan N, Markus HS. Temporal variability of asymptomatic embolization in carotid artery stenosis and optimal recording protocols. Stroke 1998;29:1129–1132.

Perednia DA, Allen A. Telemedicine technology and clinical applications. JAMA 1995;273:483–488.

Poepping TL, Nikolov HN, Rankin RN, Lee M, Holdsworth DW. An *in vitro* system for Doppler ultrasound flow studies in the stenosed carotid artery bifurcation. Ultrasound Med Biol 2002;28: 495–506.

Preston J, Brown FW, Hartley B. Using telemedicine to improve health care in distant areas. Hosp Community Psychiatry 1992; 43:25–32.

Qureshi AI, Suri MF, Ali Z, et al.. Role of conventional angiography in evaluation of patients with carotid artery stenosis demonstrated by Doppler ultrasound in general practice. Stroke 2001; 32:2287–2291.

Ramirez ML, Wong M, Sadler N, Shah PM. Doppler evaluation of bioprosthetic and mechanical aortic valves: Data from four models in 107 stable, ambulatory patients. Am Heart J 1988;115:418–425.

Ramnarine KV, Nassiri DK, Hoskins PR, Lubbers J. Validation of a new blood-mimicking fluid for use in Doppler flow test objects. Ultrasound Med Biol 1998;24:451–459.

Rickey DW, Picot PA, Christopher DA, Fenster A. A wall-less vessel phantom for Doppler ultrasound studies. Ultrasound Med Biol 1995;21:1163–1176.

Shafqat S, Kvedar JC, Guanci MM, Chang Y, Schwamm LH. Role for telemedicine in acute stroke. Feasibility and reliability of remote administration of the NIH stroke scale. Stroke 1999;30:2141–2145.

Smith JL, Evans DH, Fan L, et al.. Interpretation of embolic phenomena during carotid endarterectomy. Stroke 1995;26:2281–2284.

Smith RF, Rutt BK, Fox AJ, Rankin RN, Holdsworth DW. Geometric characterization of stenosed human carotid arteries. Acad Radiol 1996;3:898–911.

Smith RF, Rutt BK, Holdsworth DW. Anthropomorphic carotid bifurcation phantom for MRI applications. J Magn Reson Imaging 1999;10:533–544.

Spencer MP, Thomas GI, Nicholls SC, Sauvage LR. Detection of middle cerebral artery emboli during carotid endarterectomy using transcranial Doppler ultrasonography. Stroke 1990;21:415–423.

Steinman AH, Tavakkoli J, Myers JG, Cobbold RS, Johnston KW. Sources of error in maximum velocity estimation using linear phased-array Doppler systems with steady flow. Ultrasound Med Biol 2001;27:655–664.

Taylor J, Hayes-Gill BR, Crowe JA, Paull CJ. Towards multi-patient leadless and wireless cardiotocography via RF telemetry. Med Eng Phys 1998;20:764–772.

Trippi JA, Lee KS, Kopp G, Nelson D, Kovacs R. Emergency echocardiography telemedicine: An efficient method to provide 24-hour consultative echocardiography. J Am Coll Cardiol 1996;27:1748–1752.

Valton L, Larrue V, Arrue P, Geraud G, Bes A. Asymptomatic cerebral embolic signals in patients with carotid stenosis. Correlation with appearance of plaque ulceration on angiography. Stroke 1995;26: 813–815.

Viegas SF, Dunn K. Telemedicine: Practicing in the information age. Philadelphia, PA: Lippincott-Raven, 1998.

Zar JH. Biostatistical analysis. Englewood Cliffs, NJ: Prentice-Hall, Inc., 1984.